

Signal Driven Sampling and Filtering a Promising Approach for Time Varying Signals Processing

Saeed Mian Qaisar, Laurent Fesquet and Marc Renaudin

Abstract—The mobile systems are powered by batteries. Reducing the system power consumption is a key to increase its autonomy. It is known that mostly the systems are dealing with time varying signals. Thus, we aim to achieve power efficiency by smartly adapting the system processing activity in accordance with the input signal local characteristics. It is done by completely rethinking the processing chain, by adopting signal driven sampling and processing. In this context, a signal driven filtering technique, based on the level crossing sampling is devised. It adapts the sampling frequency and the filter order by analysing the input signal local variations. Thus, it correlates the processing activity with the signal variations. It leads towards a drastic computational gain of the proposed technique compared to the classical one.

Keywords—Level Crossing Sampling, Activity Selection, Adaptive Rate Filtering, Computational Complexity.

I. INTRODUCTION

THIS work is a contribution in the development of smart mobile systems. The goal is to reduce their size, cost, processing noise, electromagnetic emission and especially power consumption as they are remotely powered by batteries. This can be done by smartly reorganizing their associated signal processing theory and architecture. The idea is to combine the signal driven processing with the asynchronous circuit design in order to reduce the system processing activity.

Most of the real life signals like speech, seismic, Doppler and biological signals are time varying in nature. The spectral contents of these signals vary with time, which is a direct consequence of the signal generation process [5]. Classical systems are based on the Nyquist signal processing architectures. They do not take advantage of the input signal

local variations. These systems are highly constrained due to the Shannon sampling criterion especially in the case of low activity sporadic signals. As in such a case they cause a large number of samples without any relevant information, so a useless increase of the system activity.

This problem is resolved by employing a signal driven sampling scheme, which is sensitive to the input signal local variations [12, 17]. It is based on the principle of “level-crossing” that provides a non-uniform time repartition of the samples [1], consequently it is named as the LCSS (level crossing sampling scheme). This sampling scheme drastically reduces the activity of the post processing chain because it only captures the relevant information [11, 13]. In this context, analog to digital converters based on the LCSS have been developed [2, 4, 18]. Algorithms for processing [3, 11, 13, 24] and analysis [8, 12, 19] of the non-uniformly spaced out in time sampled data obtained with the LCSS have also been developed.

This paper focuses on the development of an efficient FIR (Finite Impulse Response) filtering technique. The idea is to extract the input signal local features and then use them to pilot the system processing activity accordingly. This idea is realised by smartly combining the features of both non-uniform and uniform signal processing tools, which promise a drastic computational gain of the proposed technique compared to the classical one.

Section II briefly reviews the LCSS. Complete functionality of the proposed filtering technique and its appealing features description are given in Section III. Section IV deals with the computational complexity and the processing error. In Section V, the proposed technique performance is evaluated for a speech signal. Section VI finally concludes the article.

II. LCSS (LEVEL CROSSING SAMPLING SCHEME)

The concept of the LCSS is not new and has been known at least since 1950s [20]. It belongs to a class of sampling schemes, which are named as the signal dependent sampling schemes like zero-crossing sampling [21], Lebesgue sampling [22], reference signal crossing sampling [23], etc.

The LCSS is a natural choice for sampling the time varying signals. It lets the signal to dictate the sampling process [17]. The non-uniformity in the sampling process represents the signal local variations [12].

Saeed Mian Qaisar has received his M.Sc degree in Electrical Engineering from INPG, France, in 2005. Currently he is a PhD candidate in Laboratory TIMA, CNRS UMR 5159, 46 Avenue Felix-Viallet, 38031 Grenoble Cedex, France (phone: +33-476574646; fax: +33-476574981; e-mail: saeed.mian-qaisar@imag.fr).

Laurent Fesquet is an associate professor at INPG and is working with Laboratory TIMA, CNRS UMR 5159, 46 Avenue Felix-Viallet, 38031 Grenoble Cedex, France (e-mail: laurent.fesquet@imag.fr).

Marc Renaudin was a professor at INPG, he is now with TIEMPO, the startup company he co-founded in July 2007, Tiempo SAS, 110 Rue Blaise Pascal, Bat Viseo – Inovallee, 38330 Montbonnot St Martin, France (e-mail: marc.renaudin@tiempo-ic.com).

In the case of LCSS, a sample is captured only when the input analog signal $x(t)$ crosses one of the predefined threshold levels [1]. The samples are not uniformly spaced in time because they depend on $x(t)$ variations as it is clear from Fig. 1.

According to [1], the sampling instants of a non-uniformly sampled signal obtained with the LCSS are defined by Equation 1.

$$t_n = t_{n-1} + dt_n \tag{1}$$

$$dt_n = t_n - t_{n-1} \tag{2}$$

Where t_n is the current sampling instant, t_{n-1} is the previous one and dt_n is the time delay between the current and the previous sampling instants (cf. Equation 2).

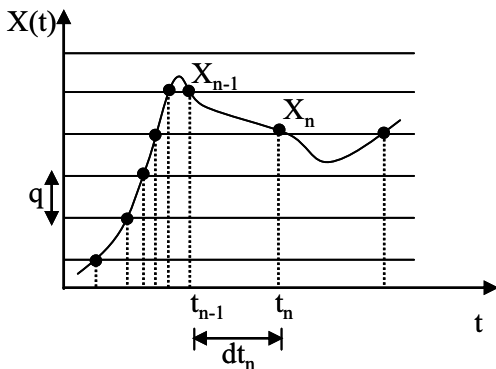


Fig. 1 Level crossing sampling scheme

III. PROPOSED SIGNAL DRIVEN FILTERING TECHNIQUE

The principle of proposed technique is represented by the block diagram, shown in Figure 2.

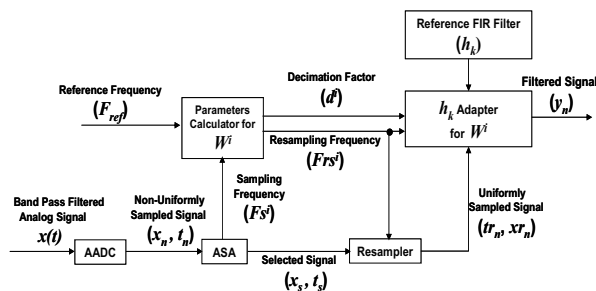


Fig. 2 Block diagram of the proposed filtering technique

The activity selection and local features extraction [8] is the base of the proposed technique. It makes to achieve the following goals.

- Adaptive rate sampling (only relevant number of samples to process)
- Adaptive rate filtering (only relevant number of operations to deliver per filtered sample).

The achievement of above defined goals assures a drastic computational gain of the proposed filtering technique compared to the classical one. The approaches to realize it are detailed in the following subsections.

A. Adaptive Rate Sampling

In the studied case, the AADC [2], is employed for digitizing $x(t)$ (cf. Figure 2). An M -bit resolution AADC has $2^M - 1$ quantization levels which are uniformly disposed according to $x(t)$ amplitude dynamics. The AADC has a finite bandwidth. Thus, to assure a proper signal capturing a band pass filter with pass-band $[f_{min}; f_{max}]$, is employed at the AADC input.

Reconstruction issue of the non-uniformly sampled signal has been discussed in [7, 14]. In [14], author showed that a bandlimited signal can be ideally reconstructed from its non-uniformly spaced samples, provided that the average number of samples satisfies the Nyquist criterion. In the case of AADC, the number of samples is directly influenced by M and the signal characteristics [2, 4, 18]. Thus, for a given application an appropriate M should be chosen in order to respect the reconstruction criterion [14].

The non-uniformly sampled signal obtained with the AADC can be used directly for further non-uniform digital processing [3, 12]. However in the studied case, the non-uniformity of the sampling process, which yields information on the signal local features, is employed to select only the relevant signal parts. Furthermore, the characteristics of each signal selected part are analyzed and are employed later on to adapt the proposed system parameters accordingly. This selection and local features extraction process is named as the ASA (Activity Selection Algorithm). The complete procedure of activity selection has been explained in [8]. The ASA displays interesting features with the AADC, which are not available in the classical case. It selects only the interesting parts of the non-uniformly sampled signal obtained with the AADC. Moreover, it correlates the length of the selected window with the signal activity, lies in it. In addition, it also provides an efficient reduction of the phenomenon of spectral leakage in the case of transient signals. This is done by avoiding the signal truncation with a simple and efficient algorithm instead of a smoothing window function, which is used in the classical scheme [8].

For a chosen M , the temporal density of the AADC sampling operation is a function of the input signal variations [11, 13, 24]. Let F_s^i represents the AADC sampling frequency for the i^{th} selected window W^i . F_s^i can be specific, depending upon the window length T_s^i in seconds and the slope of $x(t)$ part lying within this window [8]. It can be calculated by using the following equations.

$$T_s^i = t \max^i - t \min^i \tag{3}$$

$$F_s^i = \frac{N^i}{T_s^i} \tag{4}$$

In Equation 3, $tmax^i$ and $tmin^i$ are the final and the initial times of the i^{th} selected window. N^i is the number of non-uniform samples lying in W^i .

Let ΔV_{in} and $\Delta x(t)$ be the AADC and $x(t)$ amplitude dynamics respectively. In order to avail the complete AADC resolution in the studied case, $\Delta x(t)$ is always adapted to match ΔV_{in} . For a chosen M , The AADC maximum sampling frequency $F_{S_{max}}$ and minimum sampling frequency $F_{S_{min}}$ [11] are defined by Equations 5 and 6 respectively. Where, f_{max} and f_{min} are the bandwidth and the fundamental (lowest) frequencies of $x(t)$ respectively.

$$F_{S_{max}} = 2 \cdot f_{max} \cdot (2^M - 1) \quad (5)$$

$$F_{S_{min}} = 2 \cdot f_{min} \cdot (2^M - 1) \quad (6)$$

$F_{S_{max}}$ and $F_{S_{min}}$ respectively pose the upper and the lower bounds on F_{S^i} .

The selected signal lies in W^i is resampled uniformly before proceeding to the filtering stage (cf. Figure 2). Characteristics of the selected signal part lies in W^i are employed to choose its resampling frequency F_{rs^i} . Choice of F_{rs^i} is crucial and this procedure is detailed in the Section III-B. Once the resampling is done, there are Nr^i samples in W^i .

An additional error occurs due to this resampling. Nevertheless, prior to this transformation, one can take advantage of the inherent over-sampling of the relevant signal parts in the system [11, 13]. Hence, it improves the accuracy of the post resampling process [4].

The resampling process requires interpolation, which changes the properties of the resampled signal compared to the original one. The properties of the resampled signal depend upon the interpolation technique used to resample it [9, 10]. The NNRI (nearest neighbour resampling interpolation) is employed for data resampling. It is a simple interpolation method as it employs only one non-uniform observation for each resampled one. Thus, it is efficient in terms of the computational complexity. Moreover, it provides an unbiased estimate of the original signal variance, due to this reason, it is also known as a robust interpolation method [9, 10]. The detailed reasons of choosing NNRI are discussed in [8, 9, 10].

B. Adaptive Rate Filtering

It is known that for fixed design parameters (cut-off frequency, transition-band width, pass-band and stop-band ripples) the FIR filter order varies as a function of the operational sampling frequency. For high sampling frequency, the order is high and vice versa. In the classical case, the sampling frequency and the filter order both remains unique regardless of the input signal variations, so they have to be chosen for the worst case. This time invariant nature of the classical filtering causes a useless increase of the processing load. This drawback has been resolved up to a certain extent by employing the multirate filtering techniques [15, 16, 25]. They achieve computational efficiency which is not attainable

with the classical approach.

The proposed filtering technique is a smart alternative of the multirate filtering techniques. It adapts the sampling frequency and the filter order by following the input signal local variations, which leads to a drastic computational gain of the proposed technique over the classical one.

The idea is to offline design a reference FIR filter for a reference sampling frequency F_{ref} , which satisfies the Nyquist sampling criterion for $x(t)$. The process can be expressed mathematically as: $F_{ref} \geq 2 \cdot f_{max}$.

During online computation, F_{rs^i} is chosen by employing the values of F_{ref} and F_{S^i} . F_{rs^i} can be specific depending upon F_{S^i} . The reference filter impulse response h_k is sampled at F_{ref} during offline processing. Here, k is index of the reference filter coefficients. For proper online filtering F_{ref} and F_{rs^i} should match. The approaches of keeping F_{ref} and F_{rs^i} coherent are explained below.

In the case, when $F_{S^i} \geq F_{ref}$, $F_{rs^i} = F_{ref}$ is chosen and h_k remains unchanged. This choice of F_{rs^i} makes to resample the selected data which lies in W^i closer to the Nyquist rate, so avoids the unnecessary interpolations during the data resampling process. Thus, adds to the computational efficiency of the proposed techniques.

In the opposite, when $F_{S^i} < F_{ref}$, $F_{rs^i} = F_{S^i}$ is chosen and h_k is online decimated in order to reduce F_{ref} to F_{rs^i} . In this case, it appears that the data lies in W^i may be resampled at a frequency which is lesser than the Nyquist frequency of $x(t)$ and so it can cause aliasing. Since the AADC sampling frequency varies according to the slope of $x(t)$. A high frequency signal part has a high slope and the AADC samples it at a higher rate and vice versa [2, 4]. Hence, a signal part with only low frequency components can be sampled by the AADC at a sub-Nyquist frequency of $x(t)$. But still it is locally over sampled in time with respect to its local bandwidth. It is valid as far as $\Delta x(t)$ is adapted to match ΔV_{in} [11, 13]. This statement is further illustrated with the results summarized in Table 3.

In order to decimate h_k the decimation factor d^i for W^i is online calculated by employing Equation 7.

$$d^i = \frac{F_{ref}}{F_{rs^i}} \quad (7)$$

d^i can be specific for each selected window depending upon F_{rs^i} . In order to adopt an appropriate decimation process for h_k , a test is made on d^i . It is done by computing $D^i = \text{floor}(d^i)$ and verifying if $(D^i = d^i)$. Here, floor operation delivers only the integral part of d^i . If the answer is yes, then h_k is decimated with D^i , the process is clear from Equation 8.

$$h_j^i = h_{D^i \cdot k} \quad (8)$$

Equation 8 shows that the decimated filter impulse response for the i^{th} selected window h_j^i is obtained by picking every

$(D^j)^{th}$ coefficient from h_k . Here, j is index of the decimated filter coefficients. If the order of h_k is P , then the order of h_j^i is given as: $P^i = P/D^i$.

For a fractional d^i , the process of matching F_{ref} with Frs^i requires a fractional decimation of h_k , which is achieved by resampling h_k at Frs^i .

A simple decimation causes a reduction of the decimated filter energy compared to the reference one. It will lead to an attenuated version of the filtered signal. d^i is a good approximate of the ratio between the energy of the reference filter and that of the decimated one. Thus, this effect of decimation is compensated by scaling h_j^i with d^i . The process is clear from Equation 9.

$$h_j^i = d^i \cdot h_j^i \quad (9)$$

The complete flow chart of the proposed filtering technique is shown in Figure 3.

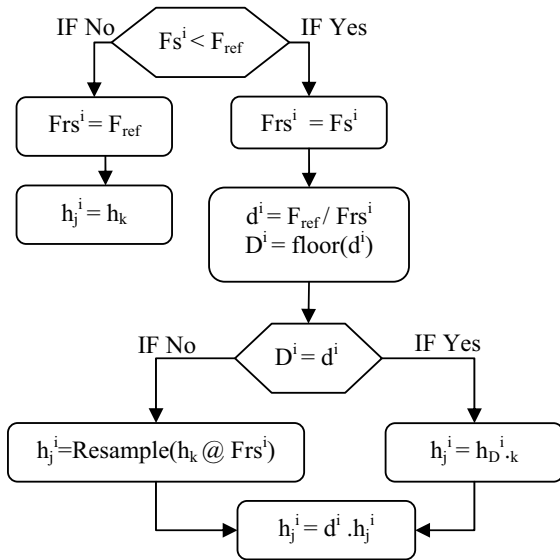


Fig. 3 Flowchart of the proposed filtering technique

C. Basic Example

In order to illustrate the ARD and the ARR filtering techniques, an input signal $x(t)$ shown on the left part of Figure 4 is employed. Its total duration is 20 seconds and it consists of three active parts. Summary of $x(t)$ activities is given in Table I.

Table I shows that $x(t)$ is band limited between $f_{min} = 5\text{Hz}$ and $f_{max} = 1\text{kHz}$. In this case, $x(t)$ is digitized by employing a 3-bit resolution AADC. Thus, for given ENOB the corresponding minimum and maximum sampling frequencies are $Fs_{min} = 70\text{Hz}$ and $Fs_{max} = 14\text{kHz}$. The AADC amplitude range $\Delta V_{in} = 1.8\text{v}$ is chosen, which results into a quantum $q = 0.2571\text{v}$.

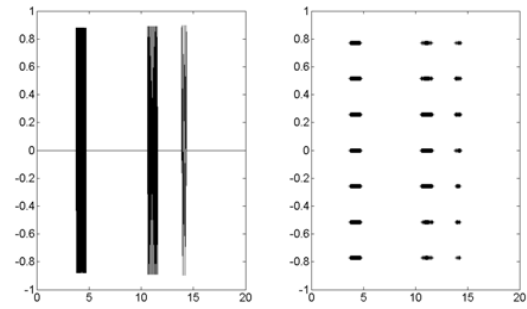


Fig. 4 Input signal (left) and the selected signal (right)

TABLE I
SUMMARY OF THE INPUT SIGNAL ACTIVITIES

ACTIVITY	SIGNAL COMPONENT	LENGTH (SEC)
1 st	$0.5 \cdot \sin(2 \cdot \pi \cdot 20 \cdot t) + 0.4 \cdot \sin(2 \cdot \pi \cdot 1000 \cdot t)$	0.5
2 nd	$0.45 \cdot \sin(2 \cdot \pi \cdot 10 \cdot t) + 0.45 \cdot \sin(2 \cdot \pi \cdot 150 \cdot t)$	1.0
3 rd	$0.6 \cdot \sin(2 \cdot \pi \cdot 5 \cdot t) + 0.3 \cdot \sin(2 \cdot \pi \cdot 100 \cdot t)$	1.0

Table I shows that $x(t)$ is band limited between 50 to 500 Hz. In this example $x(t)$ is sampled by employing a 3-bit resolution AADC. Thus, Fs_{max} and Fs_{min} become 7 kHz and 0.7 kHz respectively (cf. Equations 7, 8). $F_{ref} = 1.25\text{kHz}$ is chosen, which satisfies the criteria given in Section II-C. $\Delta V_{in} = 1.8\text{v}$ is chosen, thus q becomes 0.2571v in this case (cf. Equation 5). All $x(t)$ activities have a low and a high frequency component (cf. Table I). In order to filter out the high frequency components from each activity, a low pass reference FIR filter is implemented by employing the standard Parks-McClellan algorithm. The reference filter parameters are summarized in Table II.

TABLE II
SUMMARY OF THE REFERENCE FILTER PARAMETERS

Cut-off Freq (Hz)	Transition Band (Hz)	Pass Band Ripples (dB)	Stop Band Ripples (dB)	F_{ref} (Hz)	P
30	30~80	-25	-80	2500	127

In order to apply the ASA, the reference window length $T_{ref} = 1\text{second}$ is chosen, for this studied example [8]. The ASA delivers three selected windows, for the whole $x(t)$ span of 20 seconds. The selected signal is shown on the right part of Figure 4. The three selected windows respectively correspond to the three $x(t)$ activities. The selected window parameters are summarized in Tables III and IV.

TABLE III
SUMMARY OF THE SELECTED WINDOWS PARAMETERS

W^i	Ts^i (Sec)	N^i (smp)	Fs^i (Hz)	F_{ref} (kHz)
1 st	0.4994	3000	6000	2500
2 nd	0.9993	1083	1083	2500
3 rd	0.9986	464	464	2500

TABLE IV
SUMMARY OF THE SELECTED WINDOWS PARAMETERS

W^i	Frs^i (Hz)	d^i	Nr^i (smp)	P^i
1 st	2500	1	1250	127
2 nd	1083	2.3	1083	54
3 rd	464	5.4	464	24

Table III shows that for W^1 the case $Fs^i \geq F_{ref}$ holds, on contrary, the case $Fs^i < F_{ref}$ holds for W^2 and W^3 . The interesting features of the proposed filtering technique are evident from Tables III and IV. These are achieved due to the smart combination of the non-uniform and the uniform signal processing tools.

Fs^i represents the sampling frequency adaptation by following the local variations of $x(t)$. N^i shows that the relevant signal parts are locally over-sampled in time with respect to their local bandwidths [11, 13]. Frs^i shows the adaptation of the resampling frequency for each selected window. It further adds to the computational gain of the proposed technique by avoiding the unnecessary interpolations during the resampling process. Nr^i shows that how the adjustment of Frs^i avoids the processing of unnecessary samples during the filtering process. Ts^i exhibits the dynamic feature of ASA, which is to correlate the reference window length [8] with the signal activity lying in it. On the contrary, in the classical case, the reference window length remains static and is not able to adapt according to the signal activity lying in it. Moreover, the windowing process does not select, only the active parts of the sampled signal. For this studied example, $T_{ref} = 1$ sec would lead to twenty 1-second windows for the whole signal span (20 seconds), in the classical case. It follows that the system has to process more than the relevant information part in $x(t)$.

From Table IV, P^i represents the adaptation of h_k for W^i . It is another advantage of the proposed technique over the classical one. In the classical case, the filter remains time invariant so it has to be designed for the worst case. In this example, the input signal is band limited to 1 kHz. Therefore, if the $Fs = 2.5$ kHz is chosen in order to respect the Shannon sampling theorem. Then for the same filter parameters, summarized in Table II, Parks-McClellan design algorithm provides a 127th order filter. it makes $N=20 \times 2500 = 50000$ samples to process with the 127th order FIR filter. In the proposed technique, the total number of resampled data points is 2797. In addition, the local filters order P^2 and P^3 are lower than 127. It assures the computational efficiency of the proposed techniques compared to the classical one.

IV. PERFORMANCE EVALUATION

A. Computational Complexity

This section compares the computational complexity of the proposed filtering technique with the classical one. The complexity evaluation is made by considering the number of online operations executed to perform the algorithm.

In the classical case, for a P order FIR filter, P multiplications and P additions are required for computing each filtered sample. If N is the number of samples then the total computational complexity C_1 can be calculated by employing Equation 10.

$$C_1 = \underbrace{P \cdot N}_{\text{Additions}} + \underbrace{P \cdot N}_{\text{Multiplications}} \quad (10)$$

In the proposed filtering techniques, the adaptation process requires some extra operations for each selected window.

The choice of Frs^i requires one comparison between F_{ref} and Fs^i . The data resampling operation is also required in the proposed technique. The NNRI is employed for this purpose, which is performed as follow.

If tr_n is the n^{th} interpolation instant, which occurs between the level-crossing instants $[t_n; t_{n+1}]$. Then firstly, the distance of tr_n to each t_n and t_{n+1} is computed and secondly, a comparison among the computed distances is performed, to decide the smaller among them. It makes to choose the nearest among the level-crossing amplitudes $[x_n; x_{n+1}]$ as xr_n . Here xr_n is the n^{th} interpolated amplitude. The NNRI complexity for W^i becomes $2 \cdot Nr^i$ additions and Nr^i comparisons.

In the case, when $Fs^i < F_{ref}$, decimation of h_k is performed. In order to do so, d^i is computed by performing a division between F_{ref} and Frs^i . D^i is calculated by employing a floor operation on d^i . A comparison is made between D^i and d^i . In the case when $D^i = d^i$, the process of obtaining h_j^i is simple (cf. Figure 3). In this case, the decimator picks every $(D^i)^{\text{th}}$ coefficient from h_k . It has a negligible complexity compared to the operations like addition and multiplication. This is the reason that its complexity is not taken into account, during the complexity evaluation process.

For fractional d^i , the fractional decimation is achieved by resampling h_k at Frs^i . The resampling is performed by employing the NNRI, which performs $2 \cdot P^i$ additions and P^i comparisons to deliver h_j^i .

Finally, in order to compensate the decimation effect the decimated filter impulse response is weighted with d^i . This weighting process performs P^i multiplications. The combine computational complexity for the proposed filtering technique C_2 is given by Equation 11.

$$C_2 = \sum_{i=1}^L \left(\underbrace{\alpha}_{\text{Division}} + \underbrace{\alpha}_{\text{Floor}} + \underbrace{Nr^i + 1 + \alpha(1 + \beta P^i)}_{\text{Comparison s}} \right) + \underbrace{Nr^i (P^i + 2) + 2\alpha\beta P^i}_{\text{Additions}} + \underbrace{P^i Nr^i + \alpha P^i}_{\text{Multiplications}} \quad (11)$$

In Equation 11, $i = 1, 2, 3, \dots, L$ represents the selected windows index. α and β are the multiplying factors. α is 0 for the case when $Fs^i \geq F_{ref}$ and it is 1 otherwise. β is 0 for the case when $d^i = D^i$ and it is 1 otherwise.

From C_1 and C_2 it is clear that there are uncommon operations between both filtering techniques. In order to make them approximately comparable the following assumptions are made.

- A comparison has the same processing cost as that of an addition.
- A division or a floor has the same processing cost as that of a multiplication.

By following these assumptions, comparisons are merged into additions count and divisions plus floors are merged into multiplications count, during the complexity evaluation process. Now the Equations 11 can be written as follow.

$$C_2 = \sum_{i=1}^L \underbrace{Nr^i(P^i + 3) + 1 + \alpha(1 + 3\beta P^i)}_{\text{Additions}} + \underbrace{P^i Nr^i + \alpha(P^i + 2)}_{\text{Multiplications}} \quad (12)$$

The computational comparison of the proposed technique with the classical one is made, in terms of additions and multiplications. The respective gains for different time spans of $x(t)$ are summarized in Table V.

The computational gain of the proposed filtering technique over the classical one is calculated for results of the illustrative example, for different time spans of $x(t)$. The results are summarized in Table V.

TABLE V
SUMMARY OF THE COMPUTATIONAL GAIN

Signal Part	Gain in Additions	Gain in Multiplications
1 st activity	1.9	2.0
2 nd activity	5.3	5.4
3 rd activity	27.3	28.4
Total signal span (20)	29.4	29.8

Above results show the gain in additions and multiplications of the proposed filtering technique over the classical one. Although for the 1st activity the resampling frequency and the filter order are the same as in the classical case (cf. Table IV), yet a computational gain is achieved with the proposed filtering technique. It is due to the fact that the ASA correlates $T_{ref} = 1$ second with the signal activity (0.5 Sec.), while in the classical case T_{ref} remains static and it makes the system to process unnecessary samples. For W^2 and W^3 the gains of the proposed techniques are much larger than the classical one. It is achieved by processing the lesser number of samples at lower filter orders, in the proposed techniques compared to the classical one. While considering the total $x(t)$ span of 20 seconds, the proposed technique also take advantage of the idle $x(t)$ parts, which further adds up to their computational gains compared to the classical case.

The above results confirm that the proposed filtering techniques lead towards a drastic reduction in the number of operations compared to the classical one. This reduction in operations is achieved due to the joint benefits of the AADC, the ASA and the resampling, as they enable to adapt the sampling frequency and the filter order by following the input signal local variations.

B. Processing Error

Methods to compute the resampling and the filtering errors for the proposed technique are devised, they are detailed as follow.

In the proposed technique, the resampling error mainly contains two effects. The time-amplitude pairs uncertainties which occur due to the AADC finite timer and threshold levels precisions. The interpolation error which occurs during the uniform resampling process, by considering these two effects, the Mean resampling Error for W^i can be computed by employing the following Equation.

$$MRE^i = \frac{1}{Nr^i} \sum_{n=1}^{Nr^i} |xo_n - xr_n| \quad (13)$$

Where, xr_n is the n^{th} resampled observation, interpolated with respect to the time instant tr_n . xo_n is the original sample value which should be obtained by sampling $x(t)$ at tr_n . In the studied example discussed in Section III, $x(t)$ is analytically known, thus it is possible to compute its original samples values at any given time instant. It allows us to compute the resampling error introduced by the proposed technique by employing Equation 13. The results obtained for each selected window for the proposed technique are summarized in Table VI.

TABLE VI
MEAN RESAMPLING ERROR FOR EACH SELECTED WINDOW

Selected Window	W ¹	W ²	W ³
MRE ⁱ (dB)	-18.51	-19.63	-20.92

Table VI shows the error introduced by the proposed techniques. This process is accurate enough for a 3-bit AADC. For the higher precision applications, the resampling accuracy can be improved by increasing the AADC resolution M and the interpolation order [4, 6, 11]. Thus, an increased accuracy can be achieved at the cost of an increased computational load. Therefore, by making a suitable compromise between the accuracy level and the computational load, an appropriate solution can be proposed for a specific application.

In the proposed filtering technique, a reference filter h_k is employed and then it is online decimated for W^i depending upon the chosen Frs^i . This online decimation can causes the degradation of the filtering precision. In order to evaluate this phenomenon on our test signal, the following procedure is adapted.

A reference filtered signal is generated. In this case, instead of decimating h_k to obtain h_j^i , a specific filter h_m^i is directly designed for W^i by employing the Parks-McClellan algorithm. It is designed for Frs^i by employing the same design parameters, summarized in Table II. The corresponding signal activity is also sampled at Frs^i by employing a high precision classical ADC. This sampled signal is filtered by employing h_m^i . The filtered signal obtained in this way is used as a

reference one for W^i and its comparison is made with results obtained by the proposed technique.

Following this the mean filtering error for W^i can be calculated by employing Equation 14.

$$MFE^i = \frac{1}{Nr^i} \cdot \sum_{i=1}^{Nr^i} |y_n - \hat{y}_n| \quad (14)$$

Where, y_n is the n^{th} reference filtered sample and \hat{y}_n is the n^{th} filtered sample obtained with the proposed techniques. The mean filtering error of the proposed technique is calculated, for each selected window. The results are summarized in Table VII.

TABLE VII
MEAN FILTERING ERROR FOR EACH SELECTED WINDOW

Selected Window	W^1	W^2	W^3
MFE^i (dB)	-36.23	-23.46	-11.60

Table VII shows that the online decimation of h_k in the proposed filtering technique, causes a loss of the desired filtering quality. Indeed, the filtering error increases with the increase in d^i . The measure of this error can be used to decide an upper bound on d^i (by performing an offline calculation), for which the decimated and the scaled filter provides results with an acceptable level of accuracy. The level of accuracy is application dependent. Moreover, for high precision applications, an appropriate filter can be directly calculated online for each selected window at the cost of an increased computational load.

V. CASE STUDY

In order to evaluate the proposed technique performance for real life signals, a speech signal $x(t)$ shown on the left part of Figure 5 is employed. $x(t)$ is a 1.6 second, [50 Hz; 5 kHz] band-limited signal corresponding to a three word sentence. The goal is to determine the pitch (fundamental frequency) of $x(t)$ in order to determine the speaker's gender. For a male speaker, the pitch lies within the frequency range [100 Hz, 150 Hz], whereas for a female speaker, the pitch lies within the frequency range [200 Hz, 300 Hz] [27].

The reference frequency is chosen as $F_{ref}=11200$ Hz, which is a common sampling frequency for speech signal. A 4-bit resolution AADC is used for digitizing $x(t)$ and therefore, we have $F_{s_{min}}=1.5$ kHz and $F_{s_{max}}=150$ kHz. The amplitude range is always set to $\Delta V_{in}=1.8$ V, which leads to a quantum $q=0.12$ V. The amplitude of $x(t)$ is normalized to 0.9 V in order to avoid the AADC saturation.

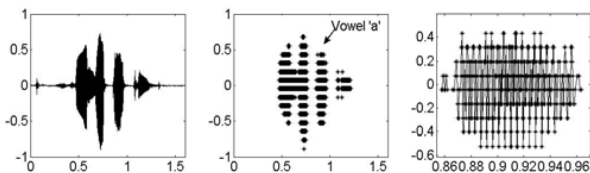


Fig. 5 Input speech signal (left), selected signal (middle) and zoom of W^2 right

The studied signal is part of a conversation and during a dialog the speech activity is 25% of the total dialog time [26]. A classical filtering system would remain active during the whole dialog duration. The proposed signal driven technique will remain active only during 25% of the dialog time, which reduces the system power consumption.

A speech signal mainly consists of vowels and consonants. Consonants are of lower amplitude compared to vowels [27]. In order to determine the speakers pitch, vowels are the relevant parts of $x(t)$. For $q=0.12$ V, the consonants are ignored during the signal acquisition process and are considered as low amplitude noise. In contrast, vowels are locally over sampled like any harmonic signal [3, 11, 13]. This smart signal acquisition further avoids the processing of useless samples, within the 25% of $x(t)$ activity and so further improves the system computational efficiency.

In order to apply the ASA, $T_{ref}=0.5$ seconds is chosen. The ASA delivers three selected windows at the output, which are shown on the middle part of Figure 5. The selected window parameters are summarized in Table VIII.

TABLE VIII
SUMMARY OF THE SELECTED WINDOWS PARAMETERS

Selected Window	T^i (Second)	N^i (Samples)	F_s^i (Hz)	F_{ref} (Hz)
W^1	0.2074	2360	11379	11200
W^2	0.1136	347	3054	11200
W^3	0.1210	265	2190	11200

Although the consonants are partially filtered out during the data acquisition process, yet for proper pitch estimation, it is required to filter out the remaining effect of high frequency consonants from $x(t)$. In this regards, a reference low pass filter is designed, by employing the standard Parks-McClellan algorithm. Its characteristics are summarized in Table IX.

TABLE IX
SUMMARY OF THE REFERENCE FILTER PARAMETERS

Cut-off Freq (Hz)	Transition Band (Hz)	Pass-band ripples (dB)	Stop-band ripples (dB)	P
300	300~400	-25	-80	284

To find the pitch, we now focus on W^2 , which corresponds to the vowel 'a'. A zoom of this signal part is plotted on the right part of Figure 5. The condition $F_s^2 < F_{ref}$ is valid and d^2 is fractional (cf. Equation 7). The adapted values of Frs^2 , Nr^2 , D^2 , and P^2 for the proposed technique are summarized in Table X.

TABLE X
ADAPTED PARAMETERS FOR W^2 IN THE PROPOSED CASE

Frs^2 (Hz)	Nr^2 (Samples)	D^2	P^2
3054	347	3.7	77

Computational gain of the proposed filtering technique compared to the classical one is computed by employing Equations 10 and 12. The results show 13.17 times gain in additions and 13.26 times gain in multiplications respectively

for W^2 . It confirms the computational efficiency of the proposed technique compared to the classical one. It is gained, firstly by achieving the smart signal acquisition and secondly by adapting the sampling frequency and the filter order by following the local variations of $x(t)$.

Spectra of the filtered signal lies in W^2 , obtained with the reference (cf. Section IV-B) and the proposed filtering techniques are plotted respectively on the right and the left parts of Figure 6.

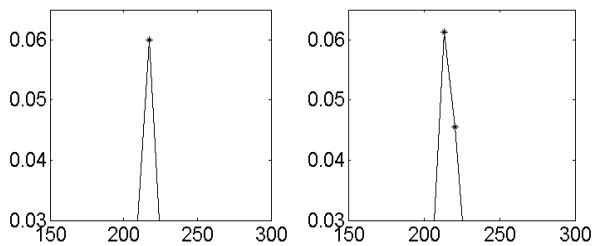


Fig. 6 Spectrum zoom of the filtered signal lies in W^2 obtained with the reference filtering (right) and the proposed filtering (left) respectively.

Spectra in Fig. 6 show that the fundamental frequency is about 215 HZ. Thus, one can easily conclude that the analyzed sentence is pronounced by a female speaker. Although it is required to decimate the reference filter 3.7 times for the proposed technique, yet the spectrum of the filtered signal, obtained with the proposed case is quite comparable to the spectrum of the reference filtered signal. It shows that even after such a level of decimation, the results delivered by the proposed techniques are of acceptable quality for the studied speech application.

VI. CONCLUSIONS

An adaptive rate filtering technique is devised. This technique is well suited for the low activity sporadic signals like electro-cardiogram, phonocardiogram, seismic signals, etc.

A reference filter is offline designed by taking into account the Nyquist sampling criterion. The complete procedure of obtaining Frs^i and h_i^i for W^i , according to the input signal variations, is described for both proposed techniques. The computational complexity of the proposed technique is deduced and compared with the classical one by employing results of the studied example. It is shown that the proposed technique results into a more than one order magnitude gain in terms of additions and multiplications over the classical one. It is achieved due to the joint benefits of the AADC, the ASA and the resampling as they enable to adapt the Fs^i , Frs^i , N^i , Nr^i , D^i and P^i by exploiting the input signal local variations, which results into a significant reduction of the total number of operations compared to the classical case. The performance of the proposed technique is also studied for a speech application. The results obtained in this case are in coherence to those obtained for the basic example.

Methods to compute the resampling and filtering errors for the proposed technique are also devised. It is shown that the errors made by the proposed technique are minor ones in the studied case. A higher precision can be achieved by increasing the AADC resolution and the interpolation order. Thus, an increased accuracy can be achieved at the cost of an increased computational load.

A detailed study of the proposed technique computational complexity, by taking into account the real processing cost at circuit level is in progress. Further research focuses on the optimization of the proposed technique and on its performance study in the case of real life applications.

REFERENCES

- [1] J.W. Mark and T.D. Todd, "A nonuniform sampling approach to data compression", IEEE Transactions on Communications, vol. COM-29, pp. 24-32, January 1981.
- [2] E. Allier, G. Sicard, L. Fesquet and M. Renaudin, "A new class of asynchronous A/D converters based on time quantization", ASYNC'03, pp.197-205, May 2003.
- [3] F. Aeschlimann, E. Allier, L. Fesquet and M. Renaudin, "Asynchronous FIR filters, towards a new digital processing chain", ASYNC'04, pp. 198-206, April 2004.
- [4] N. Sayiner, H.V. Sorensen and T.R. Viswanathan, "A Level-Crossing Sampling Scheme for A/D Conversion", IEEE Transactions on Circuits and Systems II, vol. 43, pp. 335-339, April 1996.
- [5] S.C. Sekhar and T.V. Sreenivas, "Adaptive window zero-crossing based instantaneous frequency estimation", EURASIP Journal on Applied Signal Processing, pp.1791-1806, Volume 2004, Issue 1, January 2004.
- [6] D.M. Klamer and E.Marsy, "Polynomial interpolation of randomly sampled band-limited functions and processes", SIAM Review, vol.42, No.5, pp. 1004-1019, October 1982.
- [7] F.J. Beutler, "Error free recovery from irregularly spaced samples", SIAM Review, vol. 8, pp. 328-335, 1996.
- [8] S.M. Qaisar, L. Fesquet and M. Renaudin "Spectral Analysis of a signal Driven Sampling Scheme", EUSIPCO'06, September 2006.
- [9] S. de Waele and P.M.T. Broersen, "Time domain error measures for resampled irregular data", IEEE Transactions on Instrumentation and Measurements, pp.751-756, May 1999.
- [10] S. de Waele and P.M.T. Broersen, "Error measures for resampled irregular data", IEEE Transactions on Instrumentation and Measurements, pp.216-222, April 2000.
- [11] S.M. Qaisar, L. Fesquet and M. Renaudin, "Computationally efficient adaptive rate sampling and filtering", EUSIPCO'07, pp.2139-2143, September 2007.
- [12] M. Gretains, "Time-frequency representation based chirp like signal analysis using multiple level crossings", EUSIPCO'07, pp.2154-2158, September 2007.
- [13] S.M. Qaisar, L. Fesquet and M. Renaudin, "Adaptive rate filtering for a signal driven sampling scheme", ICASSP'07, pp.1465-1468, April 2007.
- [14] F. Marvasti, "Nonuniform sampling theory and practice", Kluwer academic/Plenum Publisher, New York, 2001.
- [15] M. Vetterli, "A theory of multirate filter banks", IEEE transaction on Acoustic, Speech and Signal Processing, vol. 35, pp.356-372, March 1987.
- [16] S. Chu and C.S. Burrus, "Multirate filter designs using comb filters", IEEE transaction on Circuits and Systems, vol. 31, PP. 913-924, November 1984.
- [17] K. M. Guan and A.C. Singer, "Oppertunistic Sampling by Level-Crossing", ICASSP'07, pp.1513-1516, April 2007.
- [18] F. Akopyan, R. Manohar and A.B. Apsel, "A level-crossing flash analog-to-digital converter", ASYNC'06, pp.12-22, March 2006.
- [19] S.M. Qaisar, L. Fesquet and M. Renaudin, "An Adaptive resolution computationally efficient short time Fourier transform", EURASIP, Research Letters in Signal Processing, April 2008.
- [20] P.H. Ellis, "Extension of phase plane analysis to quantized systems", IRE transactions on Automatic Control, vol. AC (4), pp. 43-59, 1959.

- [21] F.E. Bond and C.R. Chan, "On sampling the zeros of bandwidth limited signals", IRE transactions on information theory, vol. IT-4, pp. 110-113, 1958.
- [22] K.J Astrom, B. Bernhardsson, "Comparison of Riemann and Lebesgue sampling for first order stochastic systems", Proc. Of the 41st IEEE conference on decision and control, vol 2, pp. 2011-2016, 2002.
- [23] Ivras Bilinski, "Digital alias free signal processing" John Wiley and Sons, Ltd, 2007.
- [24] S.M. Qaisar, L. Fesquet and M. Renaudin, "Computationally efficient adaptive rate sampling and filtering for low power embedded systems", SampTA'07, June 2007.
- [25] R.E. Crochiere and L.R. Rabiner, "Multirate digital signal processing", Englewood Cliffs, NJ: Prentice Hall, 1993.
- [26] P.G. Fontolliet, "Systèmes de Télécommunications", Dunod, 1983.
- [27] L.R. Rabiner and R.W. Schefer, "Digital Processing of Speech Signals", Prentice-Hall, Englewood Cliffs, New Jersey, 1978.